Mon. Not. R. Astron. Soc. **000**, 1–10 (2015) Printed 6 June 2016 (MN LATEX style file v2.2)

Galaxy-dark matter offsets in galaxy clusters and groups of the Illustris simulation

Karen Y. Ng,[1] Annalisa P. Pillepich,[2] William A. Dawson,[3] D. Wittman,[1]
Lars Hernquist,[2] etc. [order TBD]

arXiv

ABSTRACT

Galaxy clusters, which mainly compose of dark matter (DM), can be rare test beds for the particle properties of DM. However, the continuous merger and accretion events of clusters also complicate the modeling of galaxy clusters. With uncertainties coming from various modeling choices and observational constraints, we need to carefully account for the uncertainties for us to give meaningful quantitative constraints from the studies of galaxy clusters. In this paper, we test various summary statistics of the DM and the galaxy components of galaxy clusters by applying them to data from a cosmological simulation, the Illustris simulation. We examine the uncertainties of the different summary statistics, and see if the galaxy population have statistics consistent with those of the DM population. TODO: result summary. We found that the uncertainty of the offset resulting from projection effects are non-negligible and vary in unpredictable ways.

Key words: galaxy clusters, dark matter, statistics

1 INTRODUCTION

During the latest stage of structure formation, the universe gave birth to non-linear, hierarchical structures known as galaxy clusters. These clusters, made up of dark matter, galaxies and hot gas, are constantly accreting, merging and evolving with their environments. Bright galaxies that belong to a galaxy cluster or group, in particular, highlight the overdensities of the underlying dark matter (DM) distribution.

In these high density regions of the clusters, the rates of particle interactions can be enhanced, including the long-suspected self-interaction of DM particles (hereafter, SIDM). Many papers have used the DM density peaks to give constraints on the self-interaction cross sections of dark matter (Markevitch et al. 2004, Bradač et al. 2006, Mertel , Dawson, Jee etc.).

Weak and strong lensing are the most reliable methods for mapping the dark matter distribution in a galaxy cluster. Common to all the methods are the estimation of the density peaks.

We quantify the bias and uncertainty associated with the one-point summary statistic for summarizing the physical state of a galaxy cluster. Commonly used one-point statistic of galaxy clusters include: 1) papers reported using centroids but did not state what centroid that they used 2) papers used center of mass 3) papers that used peaks (Robertson et al. 2016) Offsets between different statistical measures of the galaxy and the DM population are not going to be zero.

Uncertainties affect the conclusion for the computation the hypothesis test / parameter estimation Previous work on quantifying galaxy-DM offsets included What centroids they have used

Physical motivation for using the galaxy density peak Observation footprints

Under the assumed Lambda Cold Dark Matter (ΛCDM) cosmology, it is unclear that how large the distribution offset $\Delta \boldsymbol{s}$ should be. Other complications for studying galaxy clusters arise from observation limitations. There is not a lot of information that can help constrain the line-of-sight distance of different components of a cluster.

With the advent of large-scale sky surveys, the number of identified galaxy clusters is growing quickly. Existing catalogs such as the Abell catalog also contain at least 4000 clusters with at least 30 members. The future Large Synoptic Sky Survey alone will identify over a hundred thousand galaxy clusters (CITE). It is important to verify the uncertainties associated with common summary statistics for studying galaxy clusters. Considering the large quantity of data, it is hard to use methods that require manual tuning if we want to obtain consistent statistics from the samples.

In this paper, we 1) extract realistic observables from the Illustris simulation for comparison with observations, 2) explore the pros and cons of the different statistic for summarizing the member galaxy population of a galaxy cluster, 3) give estimates for the offsets between the summary statistics of the galaxy population and the DM population, which we call

$$\Delta s \equiv \boldsymbol{s}_{\rm gal} - \boldsymbol{s}_{\rm DM}. \quad (1)$$

where $\mathbf{s_{gal}}$ and $\mathbf{s_{DM}}$ are the two dimensional (2D) spatial locations of the summary statistic of the galaxy population, and the density peak of DM respectively. Finally, we provide the distribution and investigate which quantities that are most correlated with of Δs.

The organization of this paper is as follows: In section 2, we

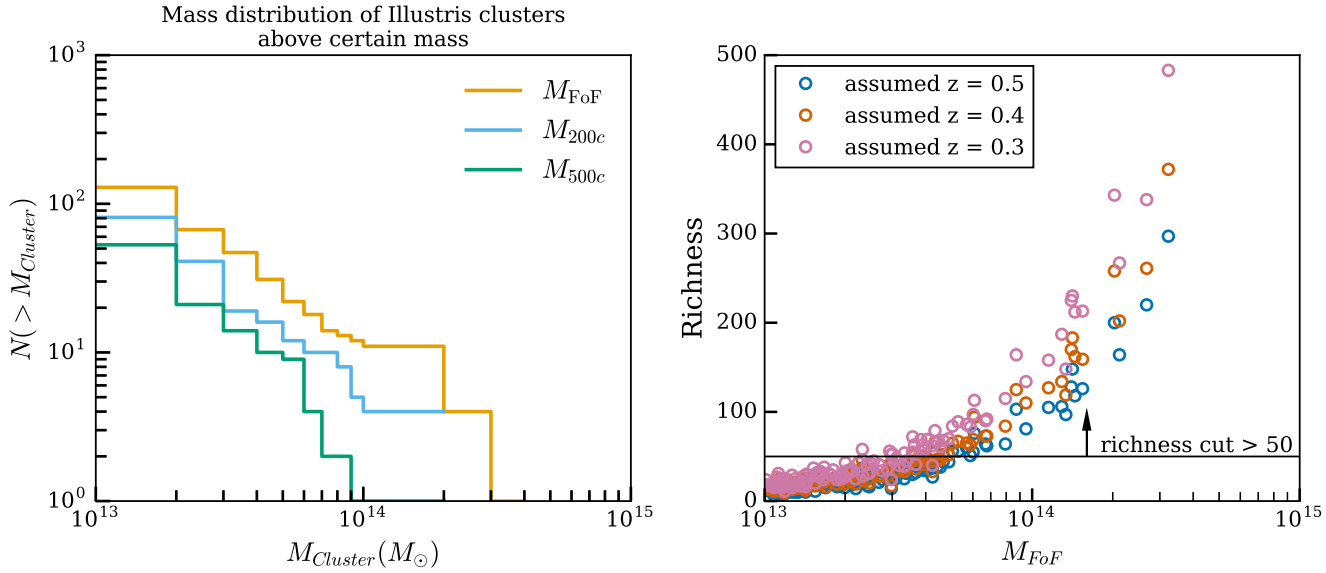

Figure 1. Left figure: Mass distribution of the group / cluster sized DM halos for different halo selection schemes. Mass estimates obtained by the FOF algorithm are labeled as M_{FoF}. Masses centered on the most bound particle within a radius those the average density is 200 or 500 times the critical density of the universe are labeled as M_{200c} and M_{500c} respectively. Discrepancies between the different measures of mass of the clusters indicate the presence of spatially separated substructures for the clusters (See Fig. 4). **Right figure:** Mass-richness relationship of galaxy clusters and groups with $M_{\rm FoF} > 10^{13} M_\odot$. We require clusters to have more than 50 member galaxies that are above observation limit, i.e. apparent $i \leq 24.4$ when we assume a cosmological redshift of $z = 0.3$, as shown by the richness cut. A total of 43 clusters have survived this cut.

will describe the physical properties of the products of the Illustris simulation (Vogelsberger et al. 2014, Genel et al. 2014), and the selection criteria that we have employed to ensure that the quantities that we examine resemble observables but without noise and systematics from observations. Then in section 3, we will describe the methods for computing various one-point statistics of the spatial distribution of galaxies how we prepare our dark matter spatial data to resemble convergence maps. We will show the comparison of the different summary statistics before we show the main results in section 4. Finally, we will discuss the implications of our results and compare it to other simulation and observations.

Our analysis makes use of the same flat Lambda Cold Dark Matter (ΛCDM) cosmology as the Illustris simulation. The relevant cosmological parameters are $\Omega_\Lambda = 0.7274, \Omega_m = 0.2726$, and $H_0 = 70.4$ km s^{-1} Mpc^{-1}.

2 THE ILLUSTRIS SIMULATION DATA

The Illustris simulation that we made use of contains some of the most realistic, simulated galaxies to date. We obtained our data from snapshot number 135 of the Illustris-1 simulation ($z = 0$). The Illustris-1 simulation has the highest particle resolution and has incorporated the most comprehensive baryonic physics among the different Illustris simulation suites. The sophisticated galaxy formation model in Illustris-1 includes star formation rate, stellar evolution due to environmental effects and supernovae feedback etc. The physics of stellar evolution were solved using a moving mesh code **AREPO** (Springel 2010). This simulation formalism accounts for the environment effects of a cluster to the evolution of galaxies. The galaxies were statistically consistent with the Sloan Digital Sky Survey data Vogelsberger et al. (2014). Since the profile of the galaxies clusters were not provided by known, symmetrical parametric forms, we can study how asymmetry in the cluster profile affects the estimate of our summary statistic. Thus, this data allows us to examine cluster galaxies in a realistic, yet noise-free way.

The catalog that maps particles to the halo of a certain cluster was created by the **Subfind** algorithm. Galaxy data: The friends-of-friends (FOF) finder (CITE properly: Davis et al. 1985) was used to identify dark matter structures. These galaxy-size halos are also referred to as subhalos, the dark matter host of what we refer to as galaxies in Illustris-1.

Data matter data: While **Subfind** was used to identify the affinity of particles

The observation bands available in the Illustris data include the u, g, r, i, z bands.

For our results, we make use of galaxy clusters / groups that have at least 50 member galaxies after this magnitude cut in the i band. This is because of the relatively large statistical uncertainty from if we try to analyze clusters with less than 50 member galaxies.

2.0.1 Cluster properties

2.1 Relaxedness of the clusters

Clusters undergo merger activities in the time scale of million of years. Observations can only provide snapshots of the state of a cluster. This info is also hard to retrieve from simulations across different saved states. We quantify the state of the cluster by providing several quantitative definitions of non-relaxedness and see how they correlate with Δs. Some definitions of non-relaxedness referred by the simulation community include:

- ratio of mass outside the dominant dark matter halo over the total mass of the galaxy cluster
- distance between the most bound particle from the center of mass as a function of R_{200c}.

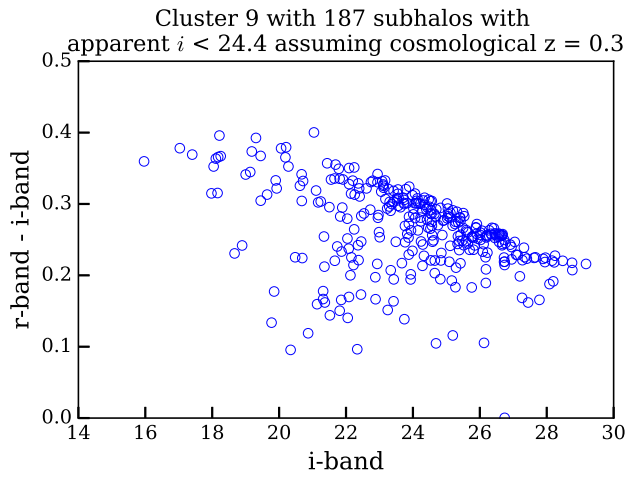

Figure 2. Color-magnitude diagram of one of the galaxy clusters that is selected for analysis. This cluster is the 9th most massive. The apparent magnitude is calculated assuming that the cosmological redshift (distance) is $z = 0.3$. We can see a clear overdense region that corresponds to a red-sequence. The color-magnitude diagrams of the other clusters can be found in the Jupyter notebook at https://goo.gl/TJmI6s.

While we try to provide more observation oriented quantities as we would discuss in the method section 3.0.2.

2.2 Selection of the field of view

As a default output from the Illustris simulation, subhalos and particles of each galaxy cluster and group are identified by the halo finder (CITE). We make use of the member particle / subhalo identification as our default volume selection scheme for each cluster / group. We understand that this choice of volume selection can be more ideal than observational conditions. We make use of this volume selection scheme for baseline comparisons.

Furthermore, assuming a conservative line-of-sight (los) distance , i.e. cosmological redshift, of $z = 0.4$, the projected extent for most of the Illustris galaxy clusters and groups, fits inside the field of view of telescopes, such as the Subaru Suprime Camera, which covers a physical area of ~ 9 Mpc $\times 7$ Mpc. Halo and FoF finding is described in (Vogelsberger et al. 2014).

2.2.1 Spatial Projections

The summary statistics are computed all based on 2D matter projections of the spatial location. In order to represent the projection uncertainty, we sample the projections evenly by using HealPy (CITE), which is a Python wrapper for HealPix (CITE). The viewing angles of the projections are defined by an elevation angle ξ and an azimuthal angle ϕ. The number of projections that we employed is FILL IN A NUMBER.

2.3 Properties of galaxies in clusters

2.3.1 Galaxy weights

Not all galaxies are created equal, so they should not be considered with equal importance for peak identification, which requires summing the the mass proxy of different galaxies. Galaxies reside in host halos with different masses and contain different stellar masses. The brightness of galaxies in a cluster are also affected by the cluster environments. For example, the star formation rates of cluster galaxies are known to be suppressed by the high concentration of intracluster medium. (CITE) One of the most common weighting schemes employed for galaxy data is to weight by the luminosity in a particular band.

3 METHODS

There are many reasonable models for summarizing the overall spatial distribution of cluster components. Each method has different uncertainties. Our goal here is to find the not to identify galaxies as parts of subcluster components, but to find the location where we expect to see the highest mass density of the DM.

Reasonable models fall under several categories, 1) mixture models, 2) basis function expansions, such as wavelet methods and 3) non-parametric estimations such as a kernel density estimation, or hierarchical clustering. Not only do the performance of the first two methods depend heavily on model parameters, the data fit also depend quite strongly on the functional form of the underlying mixture model / wavelet basis. Often times, the mixture models and wavelet bases carry strong symmetry assumptions that may not be valid for spatial modeling of hierarchically formed galaxy clusters. This is because galaxy clusters have substructures over a wide range of length scales, from galaxy scales of hundreds of pc to fraction of a Mpc. The symmetry assumption will bias the estimate of the point estimate that we are after for non-symmetric clusters.

Well known tradeoff Bias-variance tradeoff

Goal: to identify the "center" of the light distribution. Here the adopted tracers for the light distribution are the member galaxies of the cluster and groups.

We do not claim that point estimates are sufficient statistics for best representing the physical states of galaxy clusters nor the effect of self-interacting dark matter. However, we try to understand the impact of the different choices of point estimates on the estimate of Δs. We compare four ways to identify the light/galaxy centers:

(i) Centroids
(ii) KDE + peak finder
(iii) Shrinking aperture method
(iv) Brightest cluster galaxy (BCG)

We avoid any manual methods for identifying peaks for comparison purposes, scalability and reproducibility, which is a key property of science. Since all the methods listed in this paper are automated with the source code openly available, it is possible for future studies to reuse our code for comparisons. There are a number of decisions ($\sim$[TODO] ADD NUMBER) that one needs to make to determine the summary statistics. We will try to address the sensitivity of the offset due to each decision. Furthermore, a major advantage for automation is that it allows us to scale up our analysis by applying the same methods across the different snapshots of the (Illustris) simulations to examine the variability of Δs across time.

3.0.1 Centroids or center of mass

We follow the usual definition of spatial centroid as

$$\bar{\mathbf{x}} = \frac{1}{n} \sum_i \boldsymbol{x}_i. \quad (2)$$

Table 1. Selection criteria for stellar subhalos (member galaxies) for each cluster / group

Data	Selection strategy	Sensitivity	Relevant section
Field of view (FOV)	FOF halo finder	comparable to FOV of the Subaru Suprime camera	
Observed filter	i-band	consistent over the redder r, i, z bands	
Cluster richness	$i \leq 24.4$ and $z = 0.3$	sensitive to the assumed cosmological redshift of cluster and the assumed limiting magnitude of telescope	
Two-dimensional projections	even HealPix samples over half a sphere	discussed as results	

Table 2. Comparison between various methods for estimating the one-point statistics of the galaxies of a cluster

Method	One-point statistic	Sensitivity to biases	Uncertainty	Relevant section	Comment
Centroid	2D spatial averages	High	Low		
Shrinking aperture	proxy for density peak	Higher sensitivity to substructures	Medium		
Peak finding from KDE	density peak	Lower sensitivity to substructures	Higher		
Brightest cluster galaxy		Sensitive to foreground contaminants			
Most bound particle	bottom of gravitational potential well				

While the weighted centroids are just:

$$\bar{\mathbf{x}}_w = \frac{\sum_i w_i \boldsymbol{x}_i}{\sum_i w_i}, \tag{3}$$

for each spatial dimension and the weights w_i for the i-th galaxy is described in section. Centroids can be biased 1) by subcomponents from merging activities yet the centroid estimate do not provide explicit evidence for ongoing merger or accretion, 2) by the field of view.

3.0.2 *Cross-validated Kernel Density Estimation (KDE) and the peak finder*

We employed a KDE algorithm to infer a smooth density distribution of the sparse galaxies. It is known that the choice of the functional form of the smoothing kernel does not dominate the density estimate $\hat{f}$ as long as the chosen kernel is smooth (CITE). Instead we focus our effort to use cross-validation to obtain the optimal 2D smoothing bandwidth matrix for each cluster (H) for our 2D Gaussian kernel.

$$\hat{f}(\chi; H) = \frac{1}{n} \frac{1}{(2\pi)^{d/2}|H|^{1/2}} \sum_{i=1}^{n} \exp((\chi - \mathbf{x}_i)^T H^{-1} (\chi - \mathbf{x}_i)), \tag{4}$$

where the dimensionality is $d = 2$ for our projected quantities, χ represents the uniform grid points for evaluation, and $\mathbf{x_i}$ contains the spatial coordinates for each of the identified member galaxies that survived our brightness cut.

Specifically, we made use of the KDE function in the statistical package **`ks`** (CITE Duong) in the R statistical computing environment (CITE R Core Team 2014). Cross validation eliminates free parameters in the KDE and minimizes the asymptotic mean-integrated squared error (AMISE) for a best fit to the data. Although the smoothed cross validation technique takes $O(n^3)$ (DOUBLECHECK) computational requirement, the number of cluster galaxies are small enough for this method to finish quickly.

After obtaining the KDE estimate, we employed both a first and second-order finite differencing algorithm to find the local maxima. The local maxima were then sorted according to the KDE density. The density of the peaks are normalized as a fraction of the densest peak for that cluster.

Spatial location and the density of the subdominant peaks are also stored. We investigated if the presence of subdominant peaks are correlated with Δs.

3.0.3 *Shrinking aperture*

Another popular method among astronomers for finding the peak of a spatial distribution include what we call a shrinking aperture method. We test if the shrinking aperture method is able to reliably recover the densest peak. This method is dependent on the initial diameter and the initial center location of the aperture. This method does not evaluate if the cluster is made up of several components. The estimate using the shrinking aperture algorithm can be biased by substructures. The only way to inform the algorithm about substructures would be to introduce another parameter to restrict the center of the aperture, or to partition the data with another algorithm. Furthermore, the convergence rate for this iterative algorithm is not analytical and is dependent on the data. We present the convergence criteria for reference. We note that the exact implementation may result in different performances. See to BitBucket code repository

Data: subhalo that satisfy cuts as a galaxy

initial aperture centroid = mean galaxy location in each spatial dimension
distance array = euclidean distance between initial aperture center and galaxy location
aperture radius = 90th percentile of the distance array
while *(newCenterDist - oldCenterDist) / oldCenterDist* $\geq$ *2e-2* **do**
    new data array = old data array within apert
    newCenter = mean value of new data along each spatial dimension
end

Algorithm 1: Shrinking aperture algorithm. See code at https://goo.gl/nqxJl8.

for the Python implementation along with the unit test.

3.0.4 *Brightest Cluster Galaxies (BCG)*

The BCGs are formed by the merger of many smaller galaxies. The galaxy-cannibalism makes BCGs typically brighter than the rest the cluster galaxy population by several orders of magnitude. (CITE?) However, star formation can result in galaxies brighter in the bluer photometric bands. To avoid star formation from biasing our algorithm for identifying the BCG, we find at the brightest

galaxies in redder bands i.e. the r, i, z bands and found that they give consistent results for all selected clusters. The band in which we picked the BCG for presentation is the i-band.

3.1 Comparison of the methods from test data

In order to examine the statistical properties of commonly used point-estimates of the distribution of the galaxy data, we test them on data drawn from Gaussian mixtures with known mean and variance. (See Fig. 3). The main factors that affect the performance of the methods are sensitive to the statistical fluctuations of the drawn data, e.g. the spatial distribution of the data, including 1) the density profile and 2) the location(s) of subdominant mixtures, , and 3) the number of data points that we draw. It is also not enough to just compare the performance by applying each method for one realization of the data. We provide the 68% and the 95% confidence regions by applying the each method for many Monte Carlo realizations. In general, the peaks identified from the KDE density is closer to the peak of the dominant mixture (more accurate) than both the weighted centroid method and the shrinking aperture method. For example, in the bottom middle panel, it is clear that the green contours that represents the confidence region for the shrinking aperture peak is biased due to the substructure, whereas the confidence region for the centroid is so biased that it is outside the field of view of that panel. For the bottom right plot, there is also a catastrophic outlier for the shrinking aperture method for 500 data points. The outlier shows how the shrinking aperture method can have radical behavior when there are subclusters in the data.

3.2 Modeling the DM map in Illustris-1 and the lensing kernel

The most established method of inferring the projected dark matter spatial distribution from observations is through gravitational lensing. It works by detecting subtle image distortions of background galaxies due to the foreground dark matter. The resolution of the inferred map therefore depends on the properties of the galaxies, such as the projected number density, intrinsic ellipticities and morphology etc. To achieve a sufficient signal-to-noise ratio for lensing, Hoag et al. (in prep) has performed simulation for inferring the optimal size for a Gaussian smoothing kernel. In the strong lensing regime, Hoag et al. found a resolution of 11 arcseconds can best maximize the fit. This kernel translates to a physical size of [TODO] kpc assuming a cosmological redshift of [TODO] $z = 0.3$. To infer the 2D projected density from Illustris-1, we constructed (smoothed) histograms of the DM particles of each selected galaxy cluster. Physically, the 2D histogram of the dark matter of each cluster is analogous to a convergence map from a lensing analysis. We further show results after convolving the histograms with different kernel size.

3.3 Finding offsets

We computed the projected offsets between the galaxy density peaks inferred from the different peak finding methods. Furthermore, to avoid undesirable effects from setting hard boundary at offset = 0 when plotting the PDF of the offsets, we randomly assign the sign of an offset before smoothing the PDF. Finally, after smoothing the PDF, we take the

4 RESULTS

4.1 Visual inspection of galaxy clusters

From the high resolution visualization of the DM maps (2 kpc histograms) in 4, we can tell that some clusters clearly possess multiple subclusters. However, there are also several clusters with only one main component that has several peaks (galaxies) in the central region. This illustrates why finding a 'center' or peak of a cluster is an ill-defined notion. Furthermore, we show a lower-resolution visualization of the DM surface map in Fig. [TODO] compared to the higher resolution map, we can see a clear shift in the peak location. This illustrates that peak / center finding is also subject to noise from the data.

4.2 Smoothness of dark matter distribution

From the plots with peak identification, it can be shown that most clusters are multiply peaked. The actual location of these peaks also depend sensitively on the lensing kernel size and the exact reconstruction method. Ill-defined problem without a unique solution

4.3 Miscentering?

4.4 Galaxy-DM Offset in Illustris

4.4.1 Projected offsets

- those between BCG, the most bound particle and the other masses.
- explain the variation of the offsets for the same cluster under different projections

4.4.2 Correlations between the offsets and properties of the cluster / groups

- relaxedness
- mass
- richness

5 DISCUSSION

It is not easy to compare the result of this study to other study due to the differences in the multi-step method for inferring the "peak", or the "centroid".

5.1 Comparison to other simulations

5.2 Comparison to other observational studies

Central galaxy paradigm (CGP)

There are many aspects of the analysis that is not covered by this study that are performed for analyzing observational data, such as

- galaxy membership identification along the line of sight
- removal of foreground galaxies

that are important for calculating the $\sigma_{\rm SIDM}$ with using a galaxy-DM offset.

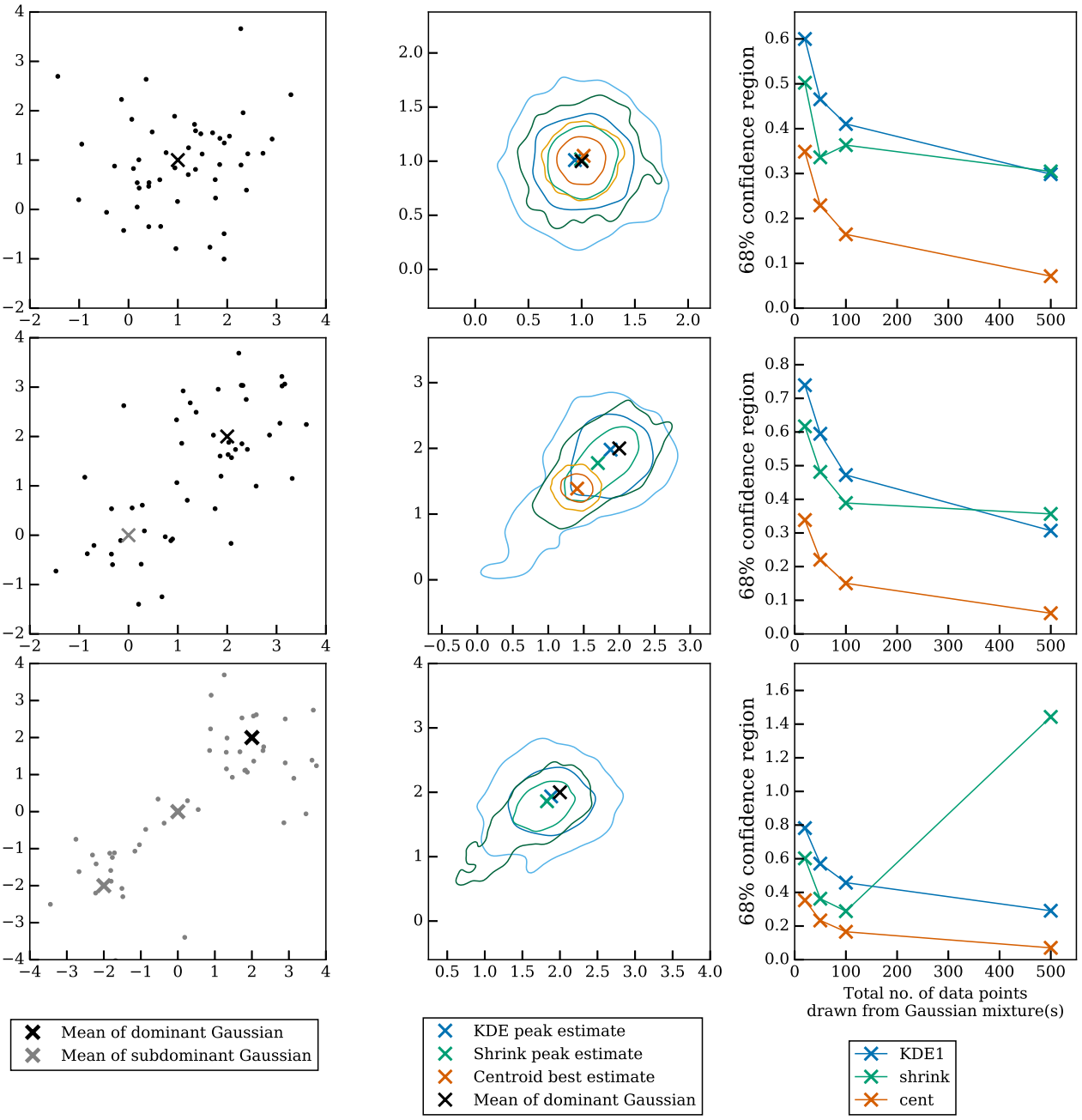

Figure 3. Comparison of peak finding performances of different methods by drawing data points (i.e. 20, 50, 100, 500) from known number of Gaussian mixtures. Panels from the top row contain data drawn from a single Gaussian mixture. The panels from the middle row contain data from two Gaussian mixtures with weight ratio = 7:3. The panels from the bottom row contain data drawn from three Gaussian mixtures with weight ratio = 55:35:10. The left column shows how 50 data points drawn from the fixed number of Gaussian mixtures look like. Due to the statistical nature of this exercise, we performed many samples to create the (68% and 95%) confidence contours of the estimates in the zoomed-in view of the data in the middle column. The rightmost column shows how the size (median contour radius) of the confidence regions vary as a function of the number of drawn data points from the Gaussian mixtures. From the middle and the rightmost column, we can tell that the KDE peak estimate is the most accurate but less precise.

5.3 Galaxy-DM Offset in Merging Galaxy Clusters

6 SUMMARY

We showed that

- the peak finding method To-be-finalized for the density of cluster galaxies is the least biased due to substructures from our test data.
- all existing peak finding methods have non-negligible uncertainty due to the small number of data points. When dealing with small number of cluster samples, the uncertainties of the peak locations should not be ignored.
- the resolution of the DM distribution can / cannot affect Δs.
- the large number of decisions that goes into computing the offsets from simulations make it hard if not impossible for comparison between studies. We call researchers in this field to make their software and analysis code openly available.

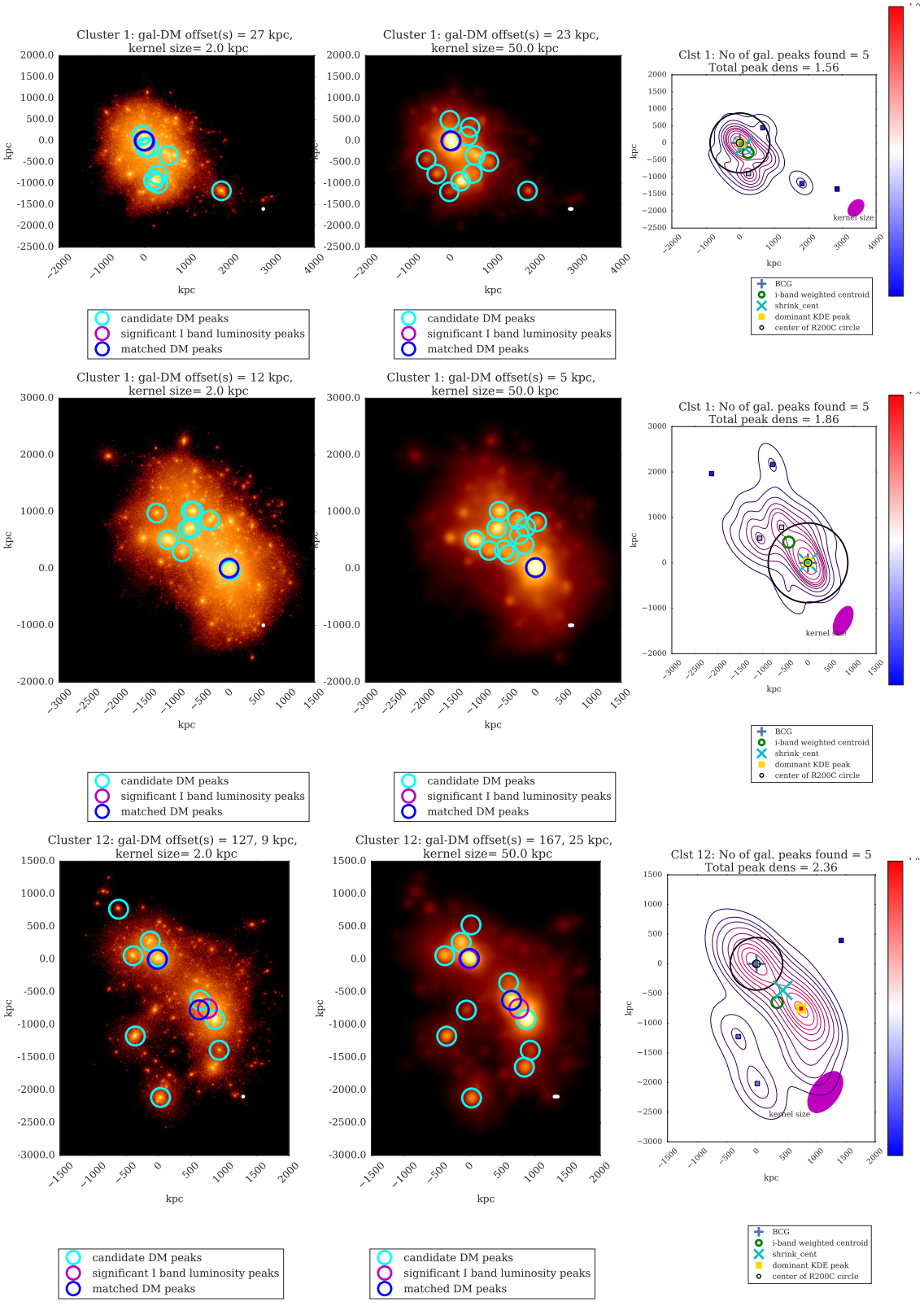

Figure 4. Visualization of clusters (each row is for the same projection of the same cluster). **Left column:** Projected density distribution of DM particle data (density overlay). The identified density peaks are indicated by colored circles. **Middle column:** The same DM projection but with treated with a 50 kpc smoothing kernel (kernel size indicated by white dot on lower right of the figure.) **Right column:** Projected galaxy kernel density estimates (KDE) of the i-band luminosity map for the member galaxies of the same clusters. See http://goo.gl/WiDijQ and http://goo.gl/89edcM for the visualization of the selected clusters inside two Jupyter notebooks.

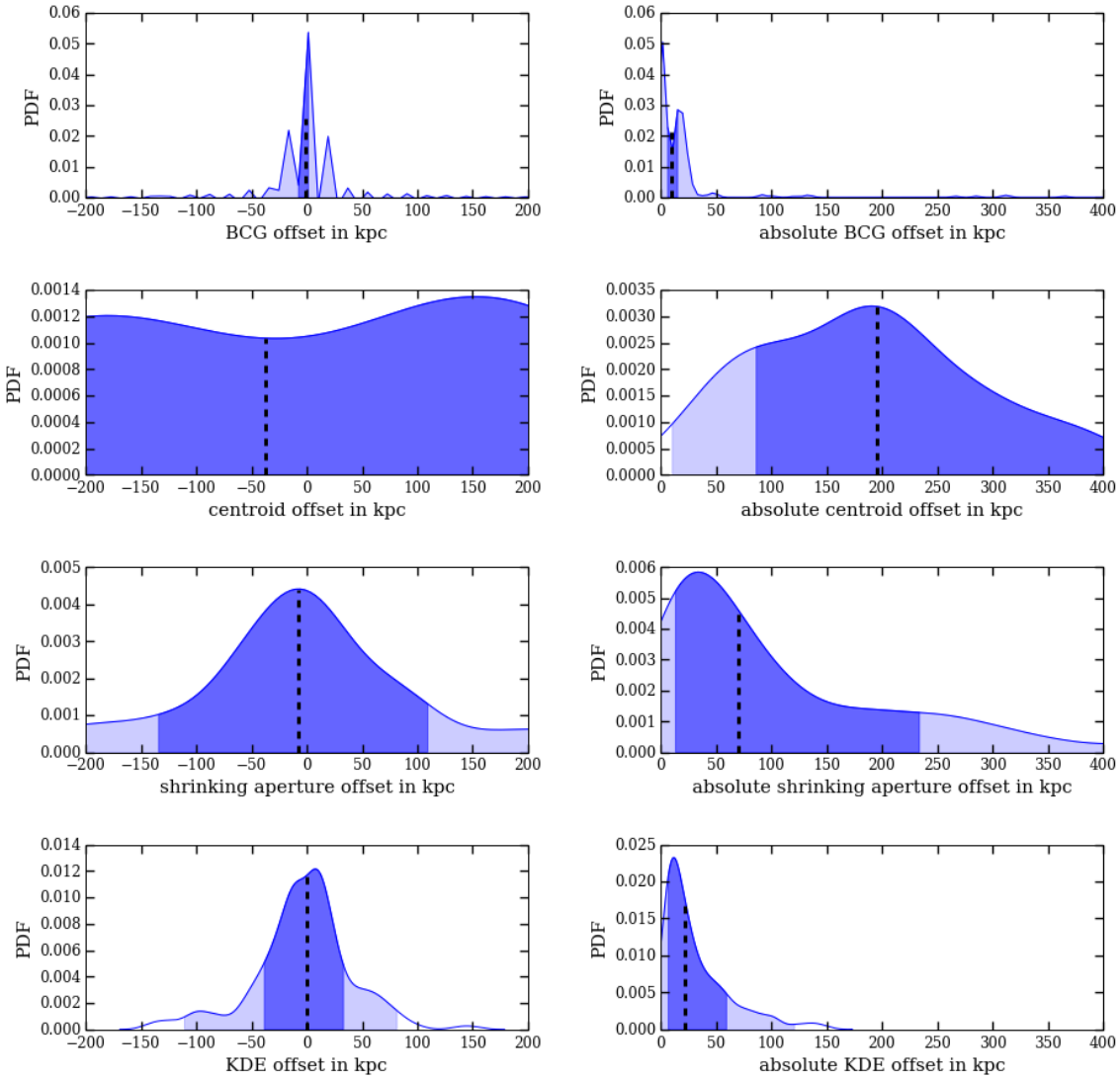

Figure 5. The distribution of different offsets of [TODO] clusters with [TODO] projections. The dark blue area indicates the 68% confidence interval while the light blue area shows the 95% confidence interval. We provide two ways of summarizing the offsets, the **left column** shows the offsets when we do not take the absolute magnitude of the offset. The estimates of the offsets on the left are all consistent with 0 within the 68% confidence interval. On the **right column**, we plot the same values after taking the absolute magnitude. The estimates from the absolute magnitude of the offsets are pushed towards larger values. None of the estimates from the absolute offsets are consistent with 0 within the 68% interval.

While this paper does not provide a solution to the complete statistical model for galaxy clusters, it points out some of the aspects that good models should incorporate, especially when the utility of studying the cluster is to constrain σ_{SIDM}.

Aspects that should be handle with care include:

- the mass profile, especially when the cluster is multimodal
- the evaluation of galaxy membership and the corresponding luminosity peak(s)
-

7 ACKNOWLEDGEMENTS

Our software setup is available through a Docker image on DockerHub while the main code are version controlled via Git and GitHub. Part of the work before the conception of this paper was discussed during the AstroHack week 2014. KN would like to thank Phil Marshall and Jake Vanderplas for preliminary discussions for analyzing galaxy clusters. Part of this work was performed under HST grant (TODO ask Dave for grant number).

REFERENCES

Bradač M., et al., 2006, ApJ, 652, 937
Genel S., et al., 2014, MNRAS, 445, 175
Markevitch M., Gonzalez a. H., Clowe D., Vikhlinin A., Forman W., Jones C., Murray S., Tucker W., 2004, ApJ, 606, 819
Robertson A., Massey R., Eke V., 2016, arXiv Prepr., p. 20
Springel V., 2010, MNRAS, 401, 791
Vogelsberger M., et al., 2014, MNRAS, 444, 1518

APPENDIX A: GETTING UNIQUE 2D PROJECTION OF THE CLUSTERS

In 3-dimensional space, rotation operations are non-commutative. We first actively rotate our clusters by the azimuthal angle ϕ before we rotate according to the elevation angle ξ. Then we project to the transformed x-y plane. With this rotation scheme, two projections are identical if

$$\begin{cases} \xi_1 + \xi_2 = \pi \\ |\phi_1 - \phi_2| = \pi \end{cases} \tag{A1}$$

It represents viewing the same cluster from opposite sides.

APPENDIX B: KERNEL DENSITY ESTIMATES

Bias variance trade-off

APPENDIX C: COLOR-MAGNITUDE DIAGRAM

This paper has been typeset from a TEX/ LATEX file prepared by the author.